İSTANBUL UNIVERSITY CERRAHPAŞA

RESEARCH ARTICLE

Electrica 2021; 21(1): 129-141

Three Speed Controllers of Direct Torque Control for a Doubly Fed Induction Motor Drive–A Comparison

Mohammed El Mahfoud[1], Badre Bossoufi[1], Najib El Ouanjli[2], Said Mahfoud[2], Mohammed Taoussi[2]

[1]Departmen of Electrical Engineering, Laboratory of Engineering Modeling and Systems Analysis, Sidi Mohamed Ben Abdellah University, Fez, Morocco
[2]Departmen of Electrical Engineering, Technologies and Industrial Services Laboratory, Higher School of Technology, Sidi Mohamed Ben Abdellah University, Fez, Morocco

Cite this article as: Mahfoud ME, Bossoufi B, Ouanjli NE, Mahfoud S, Taoussi M. Three Speed Controllers of Direct Torque Control for a Doubly Fed Induction Motor Drive–A Comparison. *Electrica,* 2021; 21(1): 129-141,

ABSTRACT

This research paper presents the performance of direct torque control (DTC) for a doubly fed induction motor (DFIM). The DFIM performance depends mainly on the design of the speed controller. The traditional proportional-integral (PI) speed controller is not very effective when the system is highly perturbed, and its gain values depend on engine parameters that are not constant. Consequently, a robust speed controller is required to achieve a high-performance drive. A backstepping speed controller is developed to achieve continuous control of the motor speed and torque. In addition, the fuzzy logic speed controller is designed to achieve high performance, speed accuracy, dynamic tracking behavior, and robustness to load disturbances. The control algorithms offered are simulated and tested in a MATLAB/Simulink environment. A comparative analysis of these speed controllers of the DTC strategy is conducted and discussed, highlighting the method that best meets the requirements in terms of dynamic response, references tracking, torque ripple, complexity, and robustness to torque variation.

Keywords: Direct torque control, doubly fed induction machine, fuzzy logic controller, proportional-integral controller, backstepping controller

Introduction

Most industrial processes extensively use electric motors to provide the drive. Depending on the application, these motors are of various types and their performance requirements are widely variable. Therefore, these motors must respond effectively to variations in setpoints (speed, position, torque).

Historically, the doubly fed induction machine is a very popular electric machine due to its high efficiency, power quality, reliability, and longevity. Particularly, DFIM is used as a variable speed generator in wind and hydroelectric power generation applications [1, 2]. It is also used in attraction systems, marine propulsion, and electric and hybrid vehicles [3, 4]. Despite these several advantages, DFIM has some disadvantages [5]:

- Very complex dynamic behavior.
- The equation system is nonlinear, multivariate, and highly coupled.
- Some of its state variables like flux are not directly measurable.

Several researchers are focusing on developing robust control techniques. Among the first techniques, the field-oriented control (FOC), introduced in the 1970s, offers a decoupling between the electromagnetic torque and flux [6]. This provides rapid torque response, a large range of speed control and high efficiency over a large range of load variation [7]. However, this control is very complex and very sensible to the parametric variations of the engine. To solve the difficulties of FOC control, TAKAHASHI developed direct torque control (DTC) in the early 1980s [8]. DTC has attracted the interest of many researchers because of its numerous advantages such as simple structure, dynamic response, and minimal dependence on ma-

Corresponding Author:
Mohammed El Mahfoud

E-mail:
Mahfoudmohammed.el@usmba.ac.ma

Received: 30.08.2020

Accepted: 30.11.2020

DOI: 10.5152/electrica.2021.20060

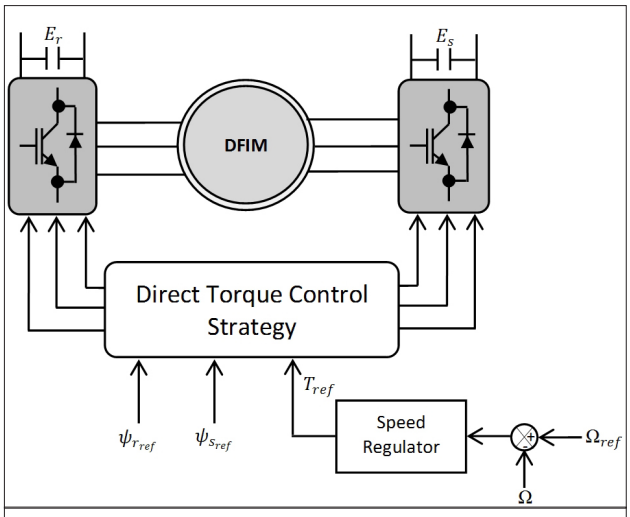

Figure 1. Overall diagram for the studied system

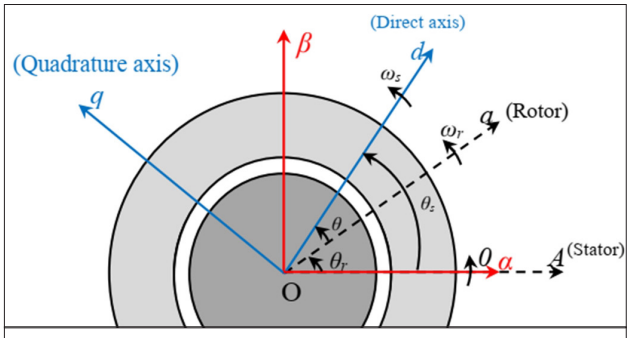

Figure 2. Spatial position of the different reference frames

chine parameters. Furthermore, it does not necessitate current regulation or coordinate transformation [9].

The hysteresis regulators and two switching tables are used to monitor the flux and electromagnetic torque of DFIM. Also, a proportional-integral controller is used in the outer loop to control the rotation speed [10]. However, the PIs are not effective when the system is very disturbed, and the controller gain values depend on the machine parameters, which are not always fixed (static) and can vary with the temperature. Therefore, a robust speed controller is desirable to achieve high-performance drive.

The contribution of this work is to improve DTC performance for a DFIM by applying robust and high-performance speed controllers. The backstepping speed regulator is developed to obtain continuous control of speed and torque of the motor. This controller involves passing from a nonlinear system to a linear system; it is based on the Lyapunov stability function. Besides, the fuzzy logic controller (FLC) based on fuzzy logic reasoning and characterized by its ability to process the imprecise, uncertain, and vague, is exploited to achieve high performance, precision of speed, dynamic tracking behavior, and robustness to load disturbances. A comparative analysis of these three speed controllers of DTC is carried out to evaluate which of these best meets the requirements.

This work is structured as follows: The dynamic model of the DFIM is presented in Section 2. Section 3 discusses the classical DTC technique based on the hysteresis comparators and switching tables. Three speed regulators of DTC strategy are designed in Section 4. The simulation results using the MATLAB/SIMULINK are presented and interpreted in Section 5. The comparative study of the three speed controllers is analyzed in Section 6. The last section of this paper lists the conclusions and recommendations for future work.

Dynamic Model of the DFIM

To develop the three-phase voltages that attack the DFIM, two voltage inverters are used: the first is connected to the stator windings and second to the rotor windings [11]. Figure 1 shows a simplified diagram of the DFIM power supply with two inverters.

The DFIM model dedicated to DTC is the two-phase model, which is expressed by the coordinates (α, β). This model minimizes the complexity of the three-phase (a, b, c) representation of the motor by the Concordia transformation [12], where the three-phase stator and rotor windings are transformed into two fictitious windings (α, β). Figure 2 illustrates the spatial arrangement of these different reference frames.

The angle θ_r represents the position of the rotor in relation to the reference axis of the stator, and the angles θ and θ_s show the relative positions of the direct axis respectively with respect to the rotor and stator axes.

With:

$$\theta_s = \theta_r + \theta \tag{1}$$

Hence, the autopilot equation is expressed as:

$$\frac{d\theta_s}{dt} = \frac{d\theta_r}{dt} + \frac{d\theta}{dt} \Rightarrow \omega_s = \omega_r + \omega \tag{2}$$

The stator and rotor voltage of DFIM in the synchronously rotating reference frame () can be expressed as [13]:

$$\begin{bmatrix} v_{s\alpha} \\ v_{s\beta} \\ v_{r\alpha} \\ v_{r\beta} \end{bmatrix} = \begin{bmatrix} R_s & 0 & 0 & 0 \\ 0 & R_s & 0 & 0 \\ 0 & 0 & R_r & 0 \\ 0 & 0 & 0 & R_r \end{bmatrix} \cdot \begin{bmatrix} i_{s\alpha} \\ i_{s\beta} \\ i_{r\alpha} \\ i_{r\beta} \end{bmatrix} + \frac{d}{dt} \cdot \begin{bmatrix} \psi_{s\alpha} \\ \psi_{s\beta} \\ \psi_{r\alpha} \\ \psi_{r\beta} \end{bmatrix} + \frac{d\theta}{dt} \cdot \begin{bmatrix} 0 \\ 0 \\ -\psi_{r\beta} \\ \psi_{r\alpha} \end{bmatrix} \tag{3}$$

The expression of the stator and rotor flux in the diphase reference frame ():

$$\begin{bmatrix} \psi_{s\alpha} \\ \psi_{s\beta} \\ \psi_{r\alpha} \\ \psi_{r\beta} \end{bmatrix} = \begin{bmatrix} L_s & 0 & M.\cos\theta & -M.\sin\theta \\ 0 & L_s & M.\sin\theta & M.\cos\theta \\ M.\cos\theta & M.\sin\theta & L_r & 0 \\ -M.\sin\theta & M.\cos\theta & 0 & L_r \end{bmatrix} \cdot \begin{bmatrix} i_{s\alpha} \\ i_{s\beta} \\ i_{r\alpha} \\ i_{r\beta} \end{bmatrix} \tag{4}$$

The electromagnetic torque can be determined from:

$$T_{em} = p.(\psi_{s\alpha}.i_{s\beta} - \psi_{s\beta}.i_{s\alpha}) \quad (5)$$

With $T_{em} = T_L + J.\frac{d\Omega}{dt} + f.\Omega$ (6)

DTC Strategy Applied to DFIM

The DTC technique for electrical motors is proposed by Takahashi o overcome the problems of the field-oriented control [14], especially sensitivity to machine parameter variation. DTC has many advantages such as less dependence on external disturbances and machine parameters, simpler implementation, and a relatively faster dynamic torque response to other controls [9]. DTC allows in the stationary frame (α, β) a decoupled control of torque and flux. A switching table is used to select a suitable voltage vector [15]. The selection of the switching states is directly proportional to the variation of the torque and flux. Therefore, the selection is made by limiting the electromagnetic torque and flux amplitudes in hysteresis regulators bands. These regulators provide separate control of these two magnitudes. Flux and torque errors are the inputs of the hysteresis controllers, and their outputs determine the appropriate voltage vector for each switching period to drive the inverter. The voltage source inverter provides eight voltage vectors, among which two are zeros.

Table 1. Voltage vectors and switch positions

	S_a	S_b	S_c
V_0	0	0	0
V_1	1	0	0
V_2	1	1	0
V_3	0	1	0
V_4	0	1	1
V_5	0	0	1
V_6	1	0	1
V_7	1	1	1

Table 2. Choice of a voltage vector

	Increase	Decrease
ψ_s or ψ_r	V_{i+1}, V_{i-1}	V_{i+2}, V_{i-2}
Tem	V_{i+1}, V_{i+2}	V_{i-1}, V_{i-2}

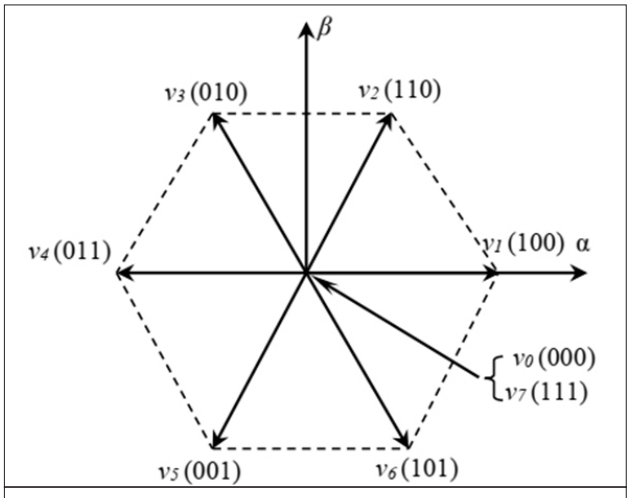

Figure 3. Voltage vectors delivered by the inverter

A switching table is used to select these vectors, based on the torque and flux errors and the position of the flux vector [12]. Table 1 shows the switching positions determining the voltage vectors.

The distribution of these vectors in the reference (α, β) is illustrated in Figure 3.

Various selection strategies for each voltage vector *V* are developed from the rules for the evolution of the electromagnetic torque and flux modulus of the DFIM, taking into account the information on the position of the flux vector in the complex plane (α, β). To delimit flux space, a partition into six zones (sectors) of 60˚ of this space is necessary. In general, when the flux (stator or rotor) is in the S_i sector, the torque and flux control can be done, as presented in Table 2.

In DTC, depending on the errors in the control variables, the switching tables indicate the positions of the inverter switches to generate the three-phase voltages that attack the DFIM. These errors are calculated by finding the difference between the estimated variable and its reference. So, the precision of the torque and flux estimation is essential to ensure good performance. Various parameters need to be determined. The rotor and stator voltages depend on the switching state, whereas the rotor and stator currents are measured. (S_a, S_b, and S_c).

The electromagnetic torque, rotor flux, and stator flux are estimated by the following equations:

$$\hat{\psi}_r = \sqrt{\hat{\psi}_{r\alpha}^2 + \hat{\psi}_{r\beta}^2} \quad (7)$$

$$\hat{\psi}_s = \sqrt{\hat{\psi}_{s\alpha}^2 + \hat{\psi}_{s\beta}^2} \quad (8)$$

$$T_{em} = p.(\hat{\psi}_{s\alpha}.i_{s\beta} - \hat{\psi}_{s\beta}.i_{s\alpha}) \quad (9)$$

With the rotor and stator flux components in the reference (α, β) is:

$$\begin{cases} \hat{\psi}_{r\alpha} = \int_0^t (v_{r\alpha} - R_r.i_{r\alpha}).dt \\ \hat{\psi}_{r\beta} = \int_0^t (v_{r\beta} - R_r.i_{r\beta}).dt \end{cases} \quad (10)$$

$$\begin{cases} \hat{\psi}_{s\alpha} = \int_0^t \left(v_{s\alpha} - R_s.i_{s\alpha}\right).dt \\ \hat{\psi}_{s\beta} = \int_0^t \left(v_{s\beta} - R_s.i_{s\beta}\right).dt \end{cases} \quad (11)$$

The rotor and stator flux positions are determined by:

$$\theta_r = arctg(\frac{\hat{\psi}_{r\beta}}{\hat{\psi}_{r\alpha}}) \quad (12)$$

$$\theta_s = arctg(\frac{\hat{\psi}_{s\beta}}{\hat{\psi}_{s\alpha}}) \quad (13)$$

The block diagram of the flux and torque estimation is presented in Figure 4.

The torque error ε_{Tem} is introduced to the three-level hysteresis regulator. The controller gives the variable (H_{Tem}= 1, 0, –1) at its output, showing the desired direction of torque development. In the same way, the flux error ε_{ψ} is introduced into a two-level hysteresis regulator, generating at its output the variable (H_{ψ} = 0,1) representing the desired flux evolution. Table 3 shows the switching table according to the variables H_{Tem} and H_{ψ}, and the sector indicating the position of the flux vector according to the principle shown in Table 2.

Figure 5 illustrates the general structure of DTC of the DFIM. The rotor and stator electromagnetic torque are controlled using a three-level hysteresis regulator, whereas the flux is controlled using a two-level hysteresis regulator. In the following section, the reference torque setpoint is preceded by a speed controller loop.

Speed Controllers

The rotation speed control is essential to ensure better tracking and good performance. Three types of speed control are discussed in this section.

Proportional-Integral controller

The proportional-integral (PI) regulator (PI) is used to control machine drives for its various advantages [16]. Indeed, it is simple, fast to implement, and allows obtaining acceptable performances [17]. That is why it has caught our attention for a study of the speed regulation system. Figure 6 shows the speed control loop using a PI regulator.

To achieve an efficient drive, the conventional PI speed controller requires an accurate mathematical model of the system and appropriate gain values of and .

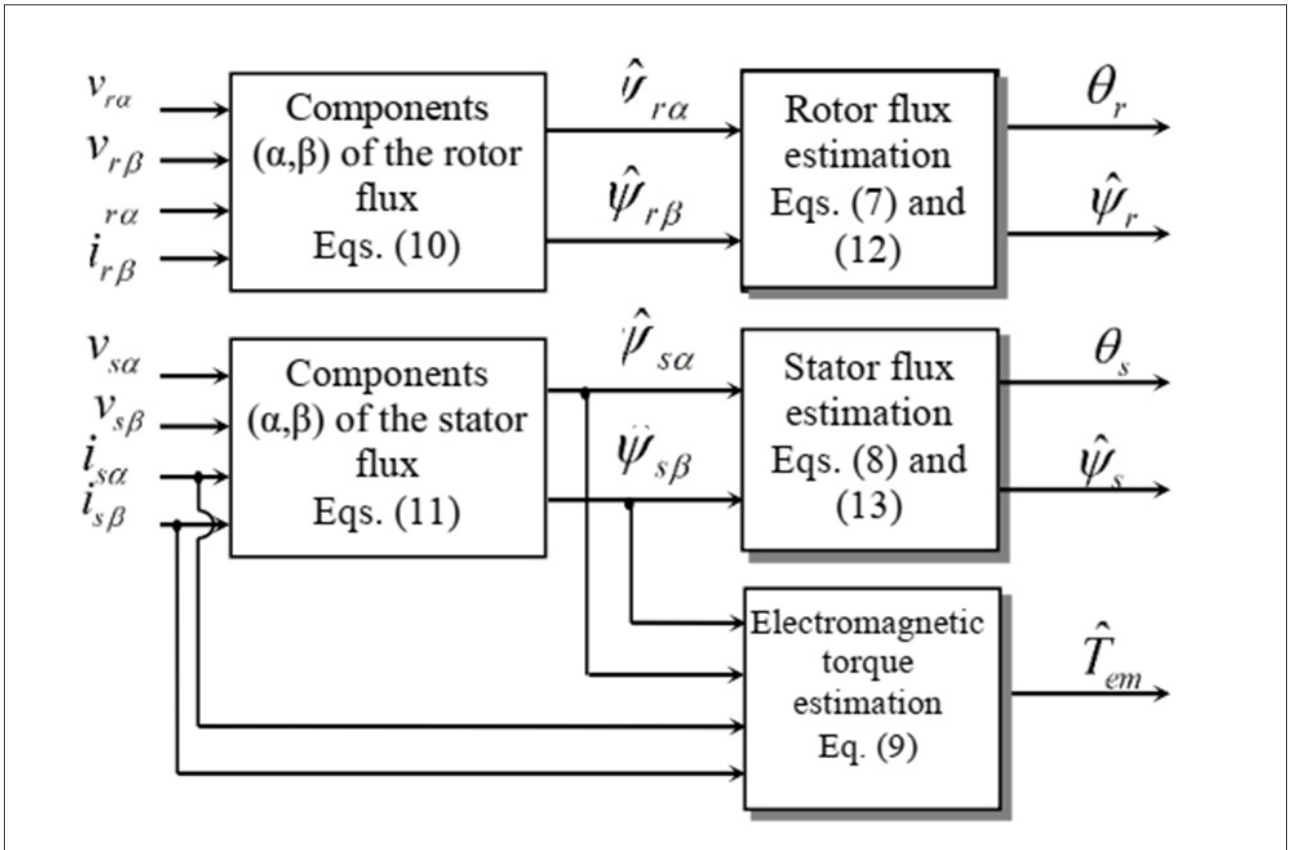

Figure 4. Block diagram of the flux and torque estimation

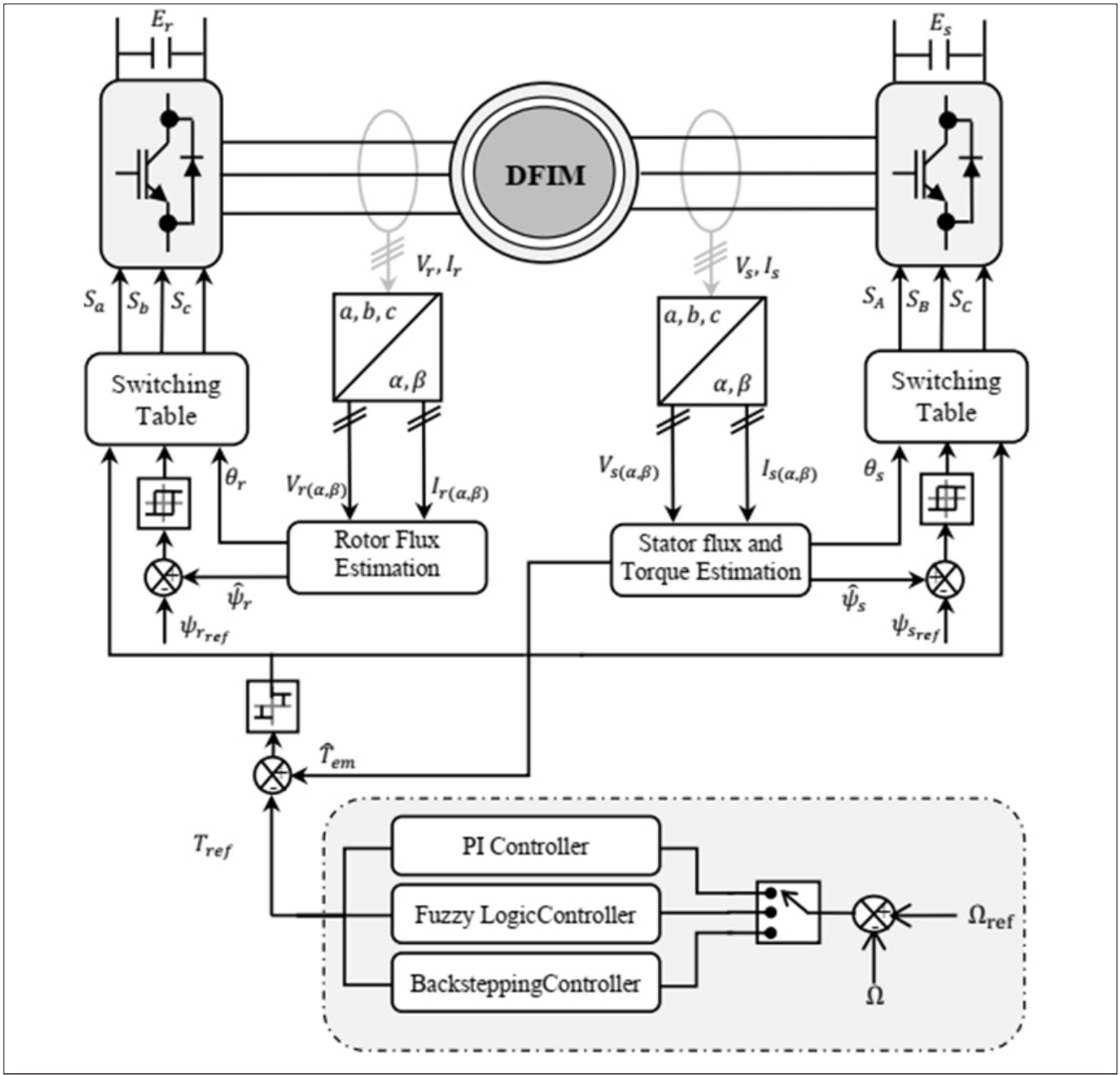

Figure 5. Synoptic schema of DTC applied to the DFIM

$$T_{em} = (k_p + \frac{k_i}{s}).\varepsilon_\Omega \quad (14)$$

Where k_i and k_p are respectively the proportional and integral gains of the IP speed controller.

Fuzzy logic controller

Fuzzy logic, or more generally the treatment of uncertainties, is one of the categories of artificial intelligence [18]. Fuzzy logic helps improve the performances of various classical control strategies applied to variable speed drives. It makes it possible to effectively obtain the law of adjustment, often without having to make thorough modeling [19]. As opposed to a standard controller or a state feedback controller, the FLC does not deal with a well-defined mathematical relationship but uses inferences with several rules based on linguistic variables.

To solve the problems of conventional controller of rotation speed, such as static error, response time, rise time, and overshoot, an FLC is proposed to control the rotation speed. The two inputs of the FLC are the speed variation and its error.

• The speed error, denoted by , is defined by:

$$\varepsilon(k) = \Omega_{ref}(k) - \Omega(k) \quad (15)$$

Table 3. Switching table

		Sector S_i					
H_{Tem}	$H_{\psi r}$ or $H_{\psi s}$	S_1 [-π/6,π/6]	S_2 [π/6,3π/6]	S_3 [3π/6,5π/6]	S_4 [5π/6,7π/6]	S_5 [7π/6,9π/6]	S_6 [9π/6,11π/6]
1	1	V_2	V_3	V_4	V_5	V_6	V_1
0		V_7	V_0	V_7	V_0	V_7	V_0
−1		V_6	V_1	V_2	V_3	V_4	V_5
1	0	V_3	V_4	V_5	V_6	V_1	V_2
0		V_0	V_7	V_0	V_7	V_0	V_7
−1		V_5	V_6	V_1	V_2	V_3	V_4

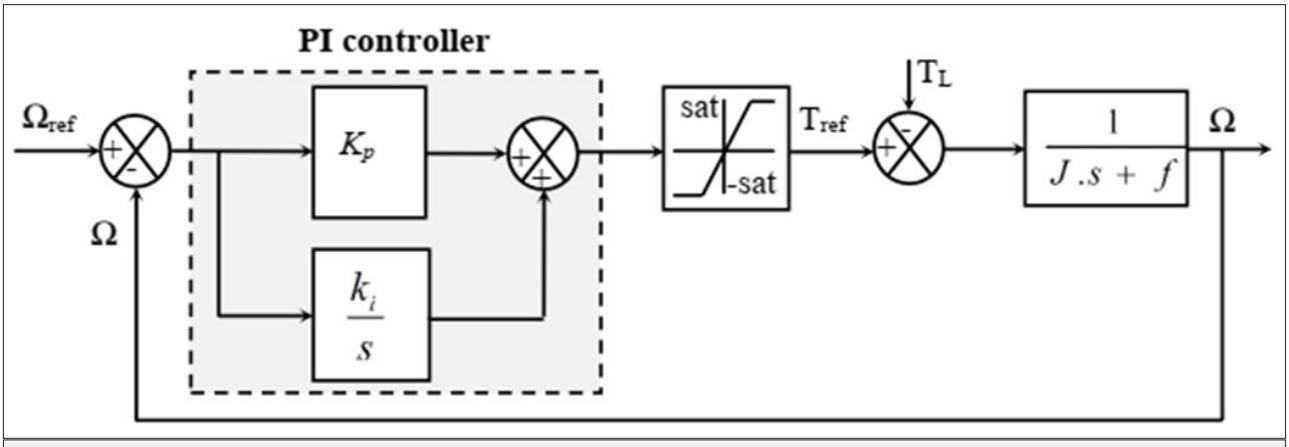

Figure 6. PI speed controller

• The variation in the speed error, denoted by Δε, is defined by:

$$\Delta\varepsilon(k) = \varepsilon(k+1) - \varepsilon(k) \tag{16}$$

The controller output corresponding to the reference torque is denoted by Δu.

The three magnitudes ε, Δε, and Δu are normalized as follows:

$$\begin{cases} E = k_1.\varepsilon \\ \Delta E = k_2.\Delta\varepsilon \\ T_{ref} = k_3.\Delta u \end{cases} \tag{17}$$

Where k_1, k_2, and k_3 are scale or standardization factors and play a decisive role in the static in addition to the dynamic performance of the control. Figure 7 shows the structure of the FLC to control the rotation speed.

The triangular and trapezoidal membership functions are used on a normalized discourse universe in the interval [−1,1] for each input and output variable, as shown in Figure 8. The fuzzy rules used to determine the output variable (reference torque variation) of the controller as a function of the input variables (error and variation error) are deduced from the inference table. In this case, the inference table consists of 25 rules, as shown in the table of Figure 8.

The decision rules are of the form: if (E is A) and (ΔE is B), then (T_{em} is C); this rule base is distributed in the form of a symmetrical diagonal decision table. For example:

- If (E is PG) and (ΔE is PG), then (T_{em} is PG).
- If (E is EZ) and (ΔE is EZ), then (T_{em} is EZ).

The above results indicate that if the speed is too low compared to its reference (E is PG), then a large torque (T_{em} is PG) is required to bring the speed back to its reference. If the speed reaches its reference and is established (E is EZ and ΔE is EZ), then keep the same torque (T_{em} is EZ).

The inference table is based on a good knowledge of the behavior of the system to be adjusted and knowledge of the control objective to be attained. The center of gravity method is chosen for defuzzification.

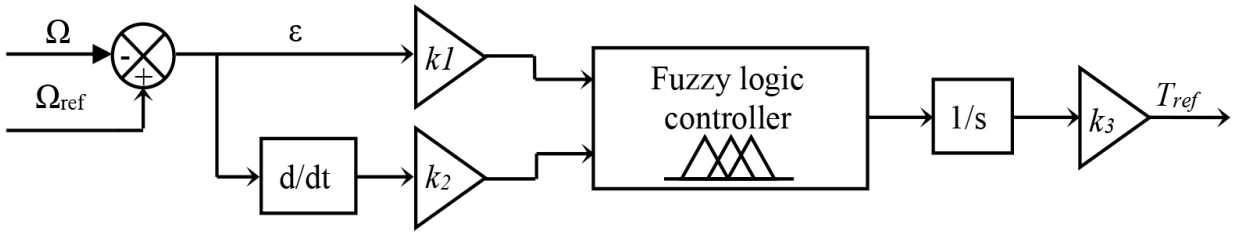

Figure 7. Structure of Fuzzy logic controller

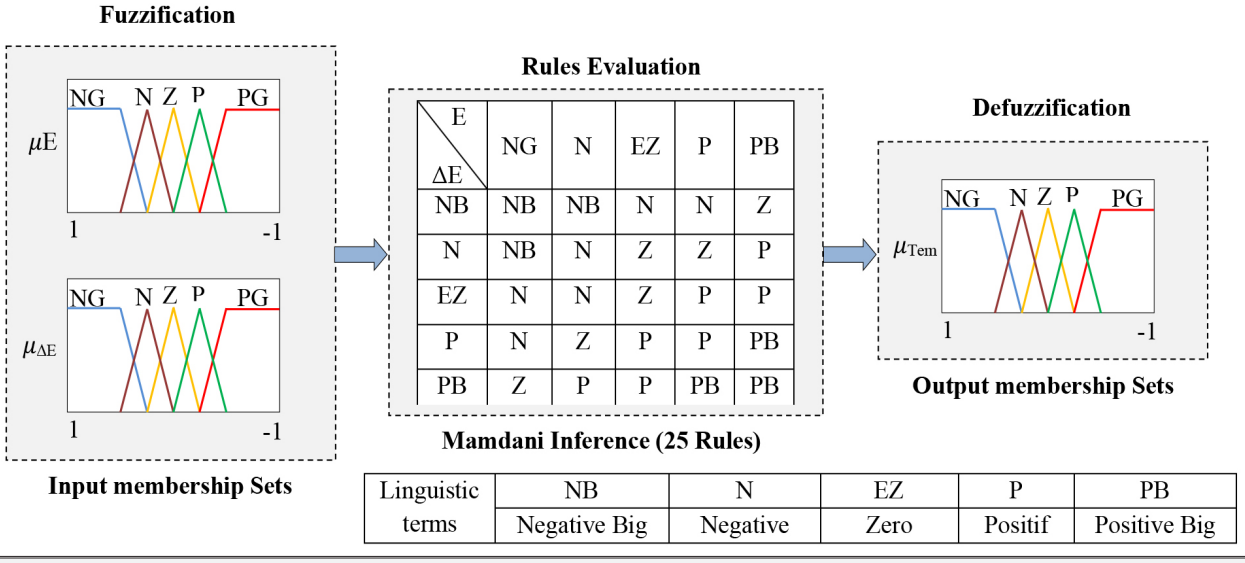

Figure 8. Internal structure of fuzzy logic controller

Backstepping controller

The aim of this method is to linearize a nonlinear system using Lyapunov's theorem [20]. It is a strong technique to test the stability of dynamic systems [21]. The implementation of this control technique for controlling the speed of DFIMs provides better performance and robustness.

From equation (6), we can write:

$$\frac{d\Omega}{dt} = \frac{1}{J}.\left[T_{em} - T_L - f.\Omega\right] \tag{18}$$

Where:

The starting point of the backstepping control is to determine the speed error:

$$e(t) = \Omega_{ref}(t) - \Omega(t) \tag{19}$$

The speed error derivative can then be shown as:

$$\dot{e}(t) = \dot{\Omega}_{ref}(t) - \dot{\Omega}(t) \tag{20}$$

Then:

$$\dot{e}(t) = \dot{\Omega}_{ref}(t) - \frac{1}{J}.T_{em} + \frac{1}{J}.T_L + \frac{f}{J}.\Omega \tag{21}$$

Subsequently, the Lyapunov function is defined in the next form:

$$V(t) = \frac{1}{2}.e^2(t) \tag{22}$$

As a result, its derivative is:

$$\dot{V}(t) = e(t).\dot{e}(t)$$
$$= e(t).\left[\dot{\Omega}_{ref} - \frac{1}{J}.T_{em} + \frac{1}{J}.T_L + \frac{f}{J}.\Omega\right] \tag{23}$$

To stabilize the system, it is important to get a negative derivative of the Lyapunov function. To do this, a positive constant "" is defined in the derivative of equation (23).

$$\dot{V}(t) = -K.\varepsilon^{2}(t) \leq 0 \quad (24)$$

From the equations (23) and (24), the controller output corresponding to the torque reference is expressed by:

$$T_{ref} = J.\left[\dot{\Omega}_{ref} + K.e\right] + f.\Omega + T_L \quad (25)$$

The block diagram of the Backstepping speed controller proposed is shown in Figure 9.

Simulation Results and Discussion

To verify the performance, robustness, and stability of the DFIM; several numerical simulation series are implemented and realized in MATLAB/Simulink. The principal characteristics of this simulation are described as shown next:

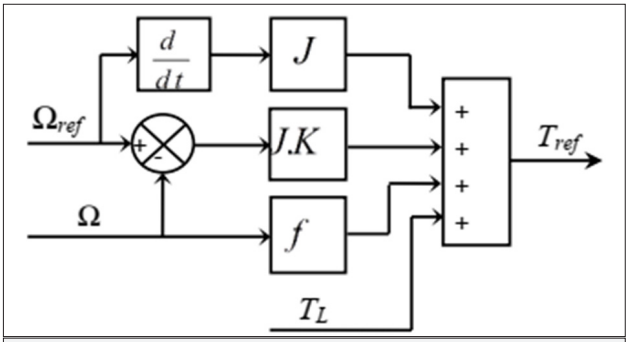

Figure 9. Backstepping speed controller

- DC bus voltages: $E_s = 300\ V$ and $E_r = 100\ V$.
- The widths of the hysteresis bands: $\Delta_{Tem} = \pm 0.01\ N.m$, $\Delta_{\psi s} = \pm 0.001\ N.m$, and $\Delta_{\psi r} = \pm 0.001\ N.m$.
- Application of a nominal load (T_L = 10 N.m) at t = 1 s.
- The DFIM parameters are mentioned in the appendix.
- The sampling frequency $f_s = 10\ kHz$.

The following figures show the simulation results obtained for different speed profiles:

- Constant speed of 157 rad/s (equivalent 1500 rpm).
- Stair profile of the rotation speed.
- Constant speed of 6 rad/s (very low speed).
- Trapezoidal speed in the reverse direction of rotation.

Figure 10 presents the simulation results for a speed step of Ω_{ref} = 157 rad/s with a load of 10N.m applied to t = 1s. The rotation speed of the three controllers follows the desired reference value, with a fast response of the fuzzy controller compared to other controllers. (The speed reaches the reference value after t_r = 0.25 s for the FLC, t_r = 0.35 s for the backstepping controller and t_r = 0.72 s for the classic PI controller). However, the speed response by the backstepping and classic PI controllers has small overshoots. Furthermore, it is observed that the torque by the fuzzy controller is less rippled compared to other regulators. The values of torque bands ΔT_{em} for each regulator are summarized in table 4. Besides, when the load torque is imposed at t = 1s, the speed is reduced (1.1 rad/s by FLC, 3 rad/s backstepping and 3.7 rad/s for classic PI). The delay time necessary to remove the disturbance impact is 5 ms faster with the fuzzy controller compared to other controllers, which shows the robustnessof the fuzzy regulator against load torque variations compared to other controllers.

In the second test, a speed staircase consisting of successive slots with amplitudes of 30, 60, 90 and 120 rad/s was tested to

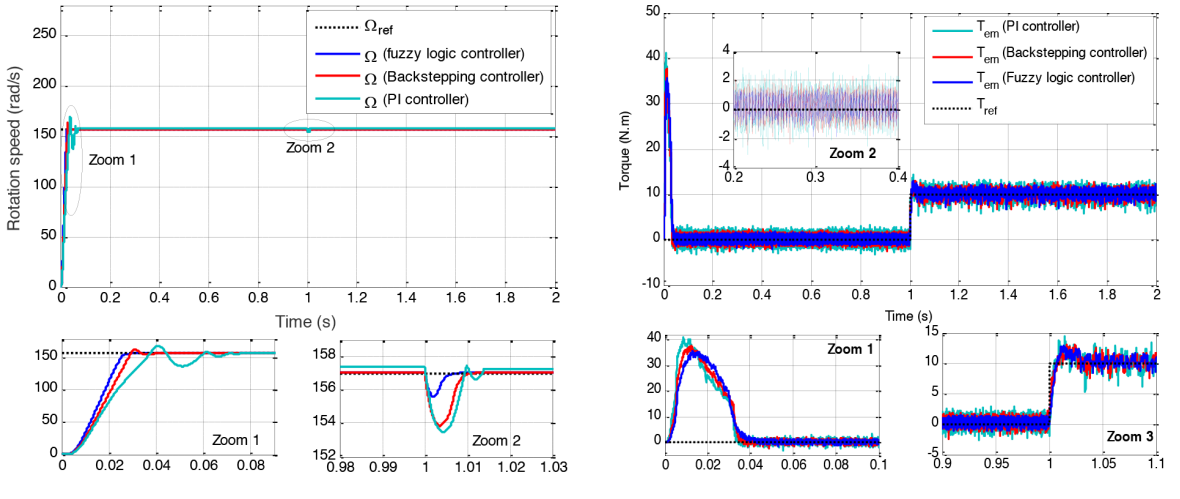

Figure 10. Constant speed response

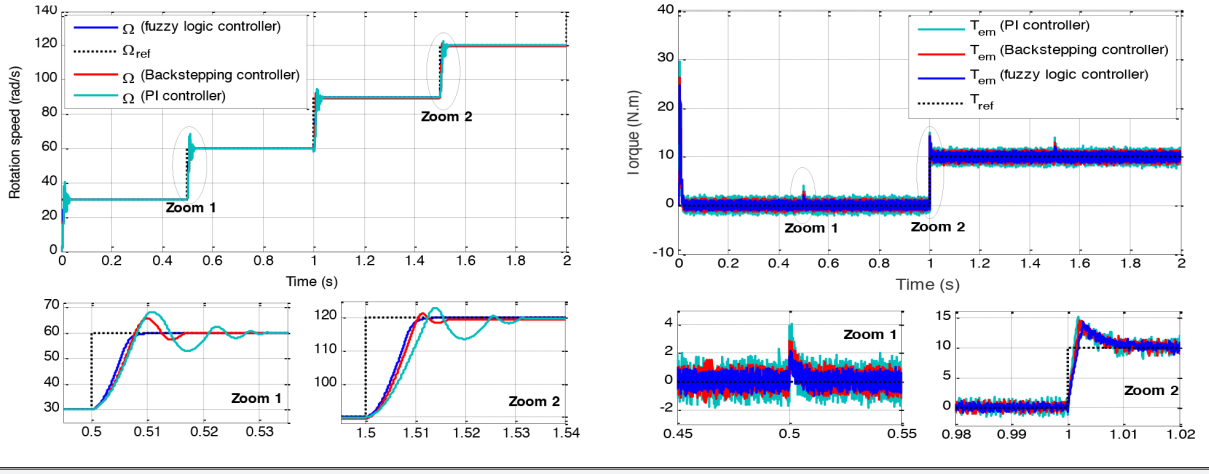

Figure 11. Response for speed staircase

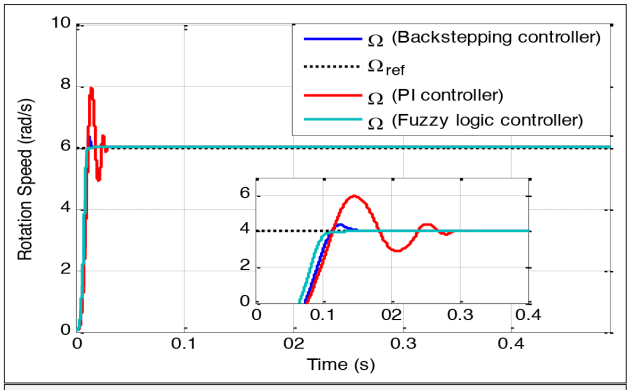

Figure 12. Very low-speed test

explore the impact of speed modification on electromagnetic torque. Figure 11 shows that the speed of rotation that follows its setpoint presents low peaks during the passage from one state to another with an overshoot (7.5% for the classic PI controller, 3.8% for backstepping, and zero for the fuzzy controller). Moreover, the torque has a few peaks during gear change. Yet, it stabilizes toward its reference value generated by each speed regulator.

Figure 12 illustrates the speed responses of the DTC with PI, Backstepping, and FLC controllers in low-speed regions. In this test, a speed reference variation has been done in 6 rad/s. The FLC-based DTC maintained good dynamics even at low-speed values contrary to the PI controller, which presents some overshot and fluctuations of the rotation speed.

The simulation results for a trapezoidal speed setpoint with rotation reversal from 157 rad/s to –157 rad/s are shown in Figure 13. The rotation speed by the FLC perfectly and quickly follows its reference value without a static or dynamic error compared to other controllers. The direction of rotation can be reversed without overshooting. Electromagnetic torque stabilizes the load torque as the speed regulators react immediately to the reference torque to accelerate or decelerate the speed. In addition, the torque marks peaks during the setpoint change and reversal of the direction of rotation.

The rotor and stator flux modules follow its references (0.5 Wb for rotor flux and 1 Wb for stator flux). These flux by fuzzy logic-based DTC have less ripples compared to other methods; they are not affected by the variation in the load and rotation speed.

The components of the rotor and stator currents for three methods are presented in Figure 13. They have a sinusoidal shape and respond well to the variations imposed by the load torque.

Comparative Study Between the Three Speed Controllers

To evaluate the influence of the control system on the dynamic and static performance of the motor, a comparison of the three speed controllers of the DTC control is analyzed. This permits to forecast the advantages and disadvantages inherent in the use of such or such controller, in addition to evaluate the method that best meets the requirements such as:

- Better system response
- Robustness to variations in torque and speed
- Less torque ripples.

Table 4 summarizes a comparison of the three speed controllers of the DTC control for the DFIM. This comparison is carried out for the same speed reference and the same load torque. It is interesting to note that the FLC used has excellent performance compared to other controllers, not only in tracking but also in regulation, with very good tracking of the reference speed and a null static error. This is applicable to all the cases of studied profiles. Moreover, the torque of the motor by the FLC is less rippled compared to other controllers. The minimization of these ripples reduces noise and mechanical vibrations, thereby guaranteeing a long engine life.

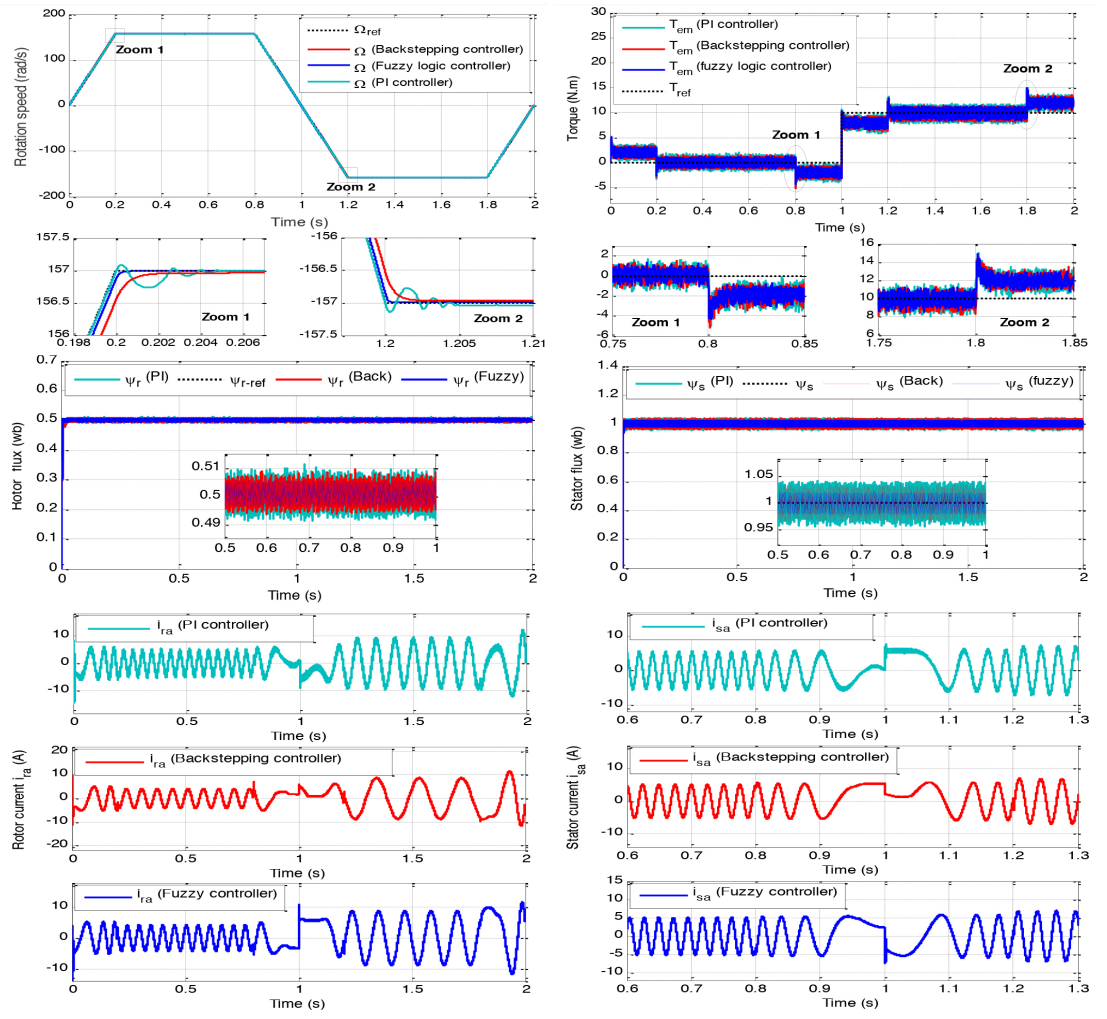

Figure 13. Trapezoidal speed response

Conclusion

This paper presents a comparative analysis of the three speed controllers of DTC applied to DFIM, a conventional proportional-integral, backstepping, and FLC. The study shows that application of the FLC to the DTC control law provides better motor performance compared to other controllers and offers several advantages such as good tracking of references, robustness, a significant reduction in torque ripples, and faster dynamic response. In conclusion, the use of the FLC with the DTC strategy results in excellent control of the drive system.

APPENDIX

Nomenclature:

$\psi_{r(\alpha,\beta)}$, $\psi_{r(\alpha,\beta)}$	: Rotor and stator flux in the reference (α,β)
$V_{r(\alpha,\beta),vs(\alpha,\beta)}$	: Rotor and stator voltages in the reference (α,β)
$i_{r(\alpha,\beta)}$, $i_{s(\alpha,\beta)}$	:Rotor and stator currents in the reference (α,β)
S_A, S_B, S_C	: Switching states
R_r, R_s	: Rotor and stator resistances
M	: Mutual inductance
L_r, L_s	: Rotor and stator inductances
J	: Moment of inertia
f	: Coefficient of viscous friction
p	: Number of pole pairs
ω_r, ω_s	: Rotor and stator pulsations
ω	: Mechanical pulsation
Ω	: Rotation speed
T_l, T_{em}	: Load and electromagnetic torque
θ_r, θ_s	: Position of the rotor and stator flux
E_r, E_s	: DC bus voltages
ε	: Speed error
$\hat{A}$	: Estimate magnitude
A_{ref}	: Reference magnitude
K_p, K_i	: Proportional gains in PI regulators

Table 4. Comparative study of the three speed regulators

Performance index		Controller design		
		PI controller	Backstepping controller	Fuzzy logic controller
Response time (ms)	157 rad/s	74	34	25
	30 rad/s	23	16	10
Rise time (ms)	157 rad/s	25	19	15
	30 rad/s	4.7	3.6	2.8
Overshot (%)	157 rad/s	7.5	3.8	0
	30 rad/s	7.5	3.8	0
Peak of electromagnetic Torque (N.m)	157 rad/s	41.2	37.6	35
	30 rad/s	29.5	26.2	24.6
Static error Ω_{ref}-Ω (%)		0.32	0.18	0.06
Fall relative for 10 N.m (%)		3.7	3	1.1
Release time for 10N.m (ms)		15	10	5
Torque ripples (N.m)		3.60	2.40	1.70
Rotor flux ripples (Wb)		0.016	0.010	0.008
Stator flux ripples (Wb)		0.083	0.065	0.041
Complexity		Simple	Simple	Complex
Robustness		Not robust	Medium	Robust

PARAMETERS OF THE DFIM

Variable	Symbol	Value (unit)
Nominal power	P_m	4 kW
Frequency	f	50 Hz
Pair pole number	P	2
Stator resistance	R_s	1.417 Ω
Rotor resistance	R_r	0.163 Ω
Maximum of mutual inductance	M	0.055 H
Stator self-inductance	L_s	0.163 H
Rotor self-inductance	L_r	0.163 H
Total inertia	J	0.066 kg.m^2
Total viscous frictions	f	0.0073 kg.m^2/s

Peer-review: Externally peer-reviewed.

Conflict of Interest: The authors have no conflicts of interest to declare.

Financial Disclosure: The authors declared that the study has received no financial support.

References

1. A. Bakouri, H. Mahmoudi, A. Abbou, "Intelligent control for doubly fed induction generator connected to the electrical network", Int. J. Power Electron. Drive Syst., vol. 7, no. 3, pp. 688-700, 2016. [Crossref]
2. B. Bossoufi, M. Karim, A. Lagrioui, M. Taoussi, A. Derouich, "Observer backstepping control of DFIG-Generators for wind turbines variable-speed: FPGA-based implementation", Renew. Energy, vol. 81, pp. 903-917, 2015. [Crossref]
3. F. Bonnet, P.E. Vidal, M. Pietrzak-David, "Direct torque control of doubly fed induction machine", Bulletin of the polish academy of sciences technical sciences, vol. 54, no. 3, pp. 307-314, 2006.
4. R. Babouri, D. Aouzellag, K. Ghedamsi, "Introduction of doubly fed induction machine in an electric vehicle", Energy Procedia, vol. 36, pp. 1076-1084, 2013. [Crossref]
5. M. Taoussi, M. Karim, B. Bossoufi, D. Hammoumi, A. Lagrioui, A. Derouich, "Speed variable adaptive backstepping control of the doubly-fed induction machine drive", Int. J. Autom. Control, vol. 10, no. 1, pp. 12-33, 2016. [Crossref]
6. M. Elmahfoud, B. Bossoufi, M. Taoussi, N. El Ouanjli, A. Derouich, "Rotor Field Oriented Control of Doubly Fed Induction Motor", 2019 Int. Conf. Optim. Appl. ICOA 2019, 2019. [Crossref]
7. N. El Ouanjli, A. Derouich, A. El Ghzizal, A. Chebabhi, M. Taoussi, "A comparative study between FOC and DTC control of the Doubly Fed Induction Motor (DFIM)", Proc. 2017 Int. Conf. Electr. Inf. Technol. ICEIT 2017, vol. 2018-Janua, pp. 1-6, 2018. [Crossref]

8. I. Takahashi, T. Noguchi, "A New Quick-Response and High-Efficiency Control Strategy of an Induction Motor", IEEE Trans. Ind. Appl., vol. IA-22, no. 5, pp. 820-827, 1986. [Crossref]
9. T. Sutikno, N. R. N. Idris, A. Jidin, "A review of direct torque control of induction motors for sustainable reliability and energy efficient drives", Renew. Sustain. Energy Rev., vol. 32, pp. 548-558, 2014. [Crossref]
10. S. K. Barik, K. K. Jaladi, "Five-Phase Induction Motor DTC-SVM Scheme with PI Controller and ANN Controller", Procedia Technol., vol. 25, no. Raerest, pp. 816-823, 2016. [Crossref]
11. N. E. Ouanjli, A. Derouich, A. E. Ghzizal, S. Motahhir, A. Chebabhi, Y. E. Mourabit, M. Taoussi, "Direct torque control of doubly fed induction motor using three-level NPC inverter," Prot. Control Mod. Power Syst., vol. 4, no. 1, 2019. [Crossref]
12. N. E. Ouanjli, A. Derouich, A. E. Ghzizal, S. Motahhir, A. Chebabhi, Y. E. Mourabit, M. Taoussi, "Modern improvement techniques of direct torque control for induction motor drives-A review", Prot. Control Mod. Power Syst., vol. 4, no. 1, 2019. [Crossref]
13. M. Taoussi, M. Karim, D. Hammoumi, C. El Bekkali, B. Bossoufi, N. El Ouanjli, "Comparative study between backstepping adaptive and field-oriented control of the DFIG applied to wind turbines", Proc. - 3rd Int. Conf. Adv. Technol. Signal Image Process. ATSIP 2017, pp. 1-6, 2017. [Crossref]
14. H. Mesloub, R. Boumaaraf, M. T. Benchouia, A. Goléa, N. Goléa, K. Srairi, "Comparative study of conventional DTC and DTC_SVM based control of PMSM motor - simulation and experimental results", Math. Comput. Simul., 2018.
15. M. Dal, "Sensorless sliding mode direct Torque Control (DTC) of induction motor", IEEE Int. Symp. Ind. Electron., vol. III, pp. 911-916, 2005. [Crossref]
16. A. Zemmit, S. Messalti, A. Harrag, "A new improved DTC of doubly fed induction machine using GA-based PI controller", Ain Shams Eng. J., vol. 9, no. 4, pp. 1877-1885, 2018. [Crossref]
17. A. Zemmit, S. Messalti, A. Harrag, "Innovative improved direct torque control of doubly fed induction machine (DFIM) using artificial neural network (ANN-DTC)", International Journal of Applied Engineering Research, Vol. 11, No. 16, pp. 9099-9105, 2016.
18. N. El Ouanjli, S. Motahhir, A. Derouich, A. El Ghzizal, A. Chebabhi, M. Taoussi, "Improved DTC strategy of doubly fed induction motor using fuzzy logic controller", Energy Reports, vol. 5, no. February, pp. 271-279, 2019. [Crossref]
19. O. Ouledali, A. Meroufel, P. Wira, S. Bentouba, "Direct torque fuzzy control of PMSM based on SVM", Energy Procedia, vol. 74, pp. 1314-1322, 2015. [Crossref]
20. S. Drid, M. Tadjine, M.-S. Nait-Said, "Robust backstepping vector control for the doubly fed induction motor", IET Control Theory and Applications, vol. 1, no. 14, pp. 861-868, 2007. [Crossref]
21. F. Mehazzem, A. Lokmane, A. Reama, D. Constantine, "Real time implementation of backstepping-multiscalar control to induction motor fed by voltage source inverter", Int. J. Hydrogen Energy, pp. 1-11, 2017. [Crossref]

Mohammed El Mahfoud was born in 1990 in Fez, Morocco. In 2013, he received Master.Sp, in Automated Industrial Systems Engineering, from Faculty of Sciences Fez University, Morocco. he is professor of physics sciences in Fez. Currently, he is pursuing Ph.D in Electrical Engineering at Faculty of Sciences, University Sidi Mohammed Ben Abdellah, Fez, Morocco. His research interests include static converters, electrical motor drives and power electronics, electrical machines control, renewable energy and artificial intelligence.

Badre Bossoufi was born in Fez city, Morocco, on May 21, 1985. He received the Ph.D. degree in Electrical Engineering from University Sidi Mohammed Ben Abdellah, Faculty of Sciences, Morocco and PhD. degree from University of Pitesti, Faculty of Electronics and Computer, Romanie and Montefiore Institute of electrical engineering, Luik, Belgium, in 2013. He was a Professor of Electrical Engineering, at the Faculty of Sciences Dhar El Mahraz, Fez, Morocco. His research interests include static converters, electrical motor drives, power electronics, Smart Grid, Renewable Energy and Artificial Intelligent.

Najib El Ouanjli was born in 1988 in Fez, Morocco. He received the Ph.D. degree in Electrical Engineering from University Sidi Mohammed Ben Abdellah, Faculty of sciences and technologies, Morocco. In 2015, he received Master.Sp, in Automated Industrial Systems Engineering, from Faculty of Sciences Fez University, Morocco. Since 2012, he is professor of physics sciences in Fez. Currently, he is pursuing Ph.D in Electrical Engineering at the Higher School of Technology, University Sidi Mohammed Ben Abdellah, Fez, Morocco. His research interests include static converters, electrical motor drives and power electronics, electrical machines control, renewable energy and artificial intelligence.

Said MAHFOUD was born in Khouribga Morocco on November 1987. He received the Licence degree in Electrical Engineering from ENSET of Mohammedia, Morocco in 2012, his Master degree from ENSET of Rabat, in 2015. He is currently working towards his PhD degree in Electrical Engineering from University Sidi Mohammed Ben Abdellah, Fez, Morocco. He is a teacher of engineering sciences option electrical sciences and technologies at the polyvalent high school in Fez. His areas of interest are Electrical Drives and Process Control, application of Intelligence techniques for control and optimize electric power systems.

Mohammed Taoussi was born in 1988 in Fez, Morocco. He received the Ph.D. degree in Electrical Engineering from University Sidi Mohammed Ben Abdellah, Faculty of Sciences, Morocco. He received his Master in Industrial Electronics from the Faculty of Sciences, Fez, in 2013. He was an Assistant Professor of Electrical Engineering, at the Higher School of technologie, Fez, Morocco. His research interests include static converters, electrical motor drives, and power electronics, smart grid, renewable energy and artificial intelligence.